Clim. Past Discuss., https://doi.org/10.5194/cp-2018-138
Manuscript under review for journal Clim. Past
Discussion started: 5 November 2018
© Author(s) 2018. CC BY 4.0 License.

Climate of the Past Discussions

Effect of precipitation seasonality on annual oxygen isotopic composition in the area of spring persistent rain in southeastern China and its palaeoclimatic implication

Haiwei Zhang[1, 2], Hai Cheng[1, 3], Yanjun Cai[2, 1], Christoph Spötl[4], and Ashish Sinha[5]

[1]Institute of Global Environmental Change, Xi'an Jiaotong University, Xi'an 710054, China

[2]Institute of Earth Environment, Chinese Academy of Sciences, State Key Laboratory of Loess and Quaternary Geology, Xi'an 710061, China

[3]Department of Earth Sciences, University of Minnesota, Minneapolis, Minnesota 55455, USA

[4]Institute of Geology, University of Innsbruck, Innsbruck 6020, Austria

[5]Department of Earth Science, California State University Dominguez Hills, Carson, California 90747, USA

Correspondence: zhanghaiwei@xjtu.edu.cn

Key Points:

- Precipitation seasonality in the SPR region in Southeast China is different from that in other monsoon regions of China.
- The ENSO modulates the precipitation seasonality in the SPR region and influences the oxygen isotopic composition of rainfall.
- Understanding the spatial differences in seasonal precipitation are key to a robust interpretation of speleothem records in the monsoon region of China.

Abstract. This study examines the seasonality of precipitation amount and $\delta^{18}O$ over the monsoon region of China (MRC). We find that the precipitation amount associated with the East Asian summer monsoon (EASM) in the spring persistent rain (SPR) region is equivalent to that of the non-summer monsoon (NSM), with the latter contributing ~50% to the amount-weighted annual $\delta^{18}O$ values in contrast with other areas of the monsoon region of China (MRC) where the $\delta^{18}O$ of annual precipitation is dominated by the EASM precipitation. The interannal relationships between ENSO index, simulated $\delta^{18}O$ data and seasonal precipitation amount in the SPR region were also analyzed. We find that on interannual timescales, less (more) EASM and more (less) NSM precipitation leading to lower (higher) EASM/NSM precipitation amount ratios result in higher (lower) precipitation $\delta^{18}O$ and consequently, in speleothems $\delta^{18}O$ during El Niño (La Niña) phases, although moisture sources and pathways may also impact this relationship. Characterizing the spatial differences in seasonal precipitation is therefore, key in correctly interpreting the speleothem $\delta^{18}O$ records from the MRC.

Key words: Precipitation seasonality, Oxygen isotope, East Asian summer monsoon, ENSO, Back-trajectory analysis

Clim. Past Discuss., https://doi.org/10.5194/cp-2018-138
Manuscript under review for journal Clim. Past
Discussion started: 5 November 2018
© Author(s) 2018. CC BY 4.0 License.

Climate of the Past Discussions
Open Access
EGU

1 Introduction

A major proportion of summertime rainfall over the monsoon region of China (MRC) is associated with the East Asian summer monsoon (EASM) (Figure 1a) (Ding, 1992). However, a significant portion of annual rainfall in southeastern China also occurs during springtime (i.e., from March until mid-May), which is known as the spring persistent rain (SPR). The SPR occurs mostly south of the middle and lower reaches of the Yangtze River (~ 24 ℃N to 30 ℃N, 110 ℃E to 120 ℃E) (Figure 1b) and is a unique synoptic and climatic phenomenon in East Asia (Tian and Yasunari, 1998; Wan and Wu, 2007, 2009). It has long been debated whether the SPR marks the onset of EASM. Ding (1992) called SPR an "early summer rainy season" and considered it as a part of the summer monsoon rainfall (Ding et al., 1994). He et al. (2008) suggested that the SPR marks the establishment of the East Asian subtropical monsoon. Other studies suggest that the SPR is unrelated to EASM rainfall and consider it as extension of winter atmospheric circulation (Tian and Yasunari, 1998; Wan and Wu, 2009). Wang and Lin (2002) suggested that the SPR over southeastern China is not a part of the EASM, because the large-scale circulation and rain-bearing systems differ from those associated with summer monsoon rainfall. Tian and Yasunari (1998) suggest that the SPR is the effect of the land-sea thermal contrast unrelated to topographical effects, as there is a coherent increase of the spring rain from southeastern China to southern Japan. Wan et al. (2008a, 2009) proposed that the formation of SPR is primarily influenced by the mechanical and thermal forcing of the Tibetan Plateau. Without this topographic element, the SPR rain belt would not exist. Climatic factors from the mid-high latitudes and the tropics also influence the interannual variability of the SPR (Feng and Li, 2011; Wu and Kirtman, 2007; Wu and Mao, 2016).

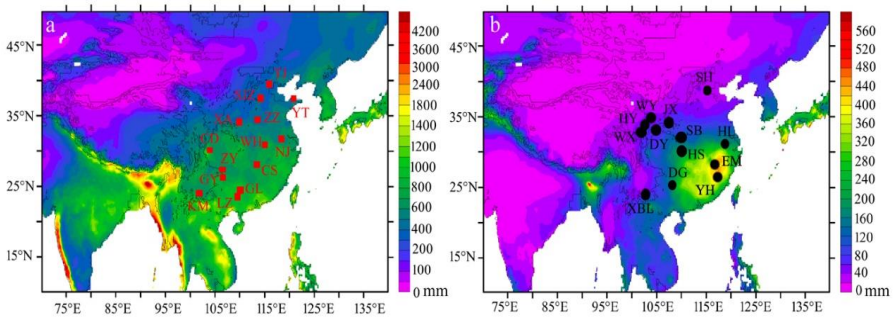

Figure 1. Overview map showing the spatial distribution of seasonal precipitation amount in China and other locations mentioned in this study. (a) Distribution of mean EASM (May-September) precipitation amount (mm/month) in China from 1951 to 2007. The red squares and the corresponding red labels show the locations of GNIP stations (TJ-Tianjin, YT-Yantai, SJZ-Shijiazhuang, XA-Xi'an, ZZ-Zhengzhou, NJ-Nanjing, WH-Wuhan, CS-Changsha, CD-Chengdu, ZY-Zunyi, GY-Guiyang,

Clim. Past Discuss., https://doi.org/10.5194/cp-2018-138
Manuscript under review for journal Clim. Past
Discussion started: 5 November 2018
© Author(s) 2018. CC BY 4.0 License.

Climate of the Past Discussions
Open Access
EGU

GL-Guilin, LZ-Liuzhou, KM-Kunming). (b) Distribution of mean SPR (March-April) precipitation amount (mm/month) in China from 1951 to 2007. The SPR is obvious in southeastern China from about 24 °N to 30 °N, and from 110 °E to 120 °E. The black circles and the corresponding black labels show the locations of caves with published stalagmite records (SH-Shihua cave, HL-Hulu cave, SB-Sanbao cave, HS-Heshang cave, DG-Dongge cave, XBL-Xiaobailong cave, WY-Wuya cave, DY-Dayu cave, WX-Wanxiang cave, HY-Huangye cave, EM-E'mei cave, YH-Yuhua cave). Precipitation data source: APHRODITE (Asian Precipitation-Highly-Resolved Observational Data Integration Towards Evaluation of Water Resources, APHRO_MA_V1101R2 product, (21)) (Yatagai et al., 2009).

Although a considerable emphasis has been placed on understanding the causes and the mechanisms of SPR, we know little about its $\delta^{18}O_p$ variability and mechanisms that produce this variability (Tan, 2016; Zhang, 2014). Based on the rainfall-monitoring data from eight sites in EASM region, Tan et al. (2016) found that, in 2012 AD, the spring rainfall amount is equivalent to the summer rainfall but their $\delta^{18}O_p$ values are different. They suggest that the seasonal $\delta^{18}O_p$ variability is affected by the changes of moisture source but not the precipitation amount variations. Some researchers studied the $\delta^{18}O_p$ variability in Changsha station where located in the SPR region and its relationship with El Niño-Southern Oscillation (ENSO) (Figure 1a) (e.g., Huang et al., 2017; Wu et al., 2015), however, they did not focus on the $\delta^{18}O_p$ variability of SPR. A better understanding of the $\delta^{18}O_p$ variability in the SPR region on seasonal to interannual scales, however, is crucial for a robust interpretation of the oxygen isotopic data of Chinese speleothems ($\delta^{18}O_s$) from this region (e.g., Cai et al., 2015; Cheng et al., 2009, 2016; Wang et al., 2001, 2008; Yuan et al., 2004; Zhang et al., 2008). Several mechanisms including the amount effect, moisture source/pathway, winter temperature, and rainfall seasonality have been shown to influence the $\delta^{18}O_p$ and $\delta^{18}O_s$ to various degrees and at different timescales (Caley et al., 2014; Clemens et al., 2010; Dayem et al., 2010; Maher, 2008, 2016; Maher and Thompson, 2012; Pausata et al., 2011; Tan, 2016). The SPR region is located within the area of the EASM and its rainy season includes both summertime monsoon rainfall and SPR (Wan and Wu, 2009), therefore, the dynamical mechanisms that influence the $\delta^{18}O_p$ in this region are likely complex. The aim of this study is to examine this climate-proxy relationship during the instrumental period. To this end, we compare the seasonal variations of precipitation amount and $\delta^{18}O_p$ in the SPR region with other regions of the MRC and discuss the interannual variations of precipitation amount and $\delta^{18}O_p$ in the SPR region and their relationship with the large-scale oceanic-atmospheric circulation.

Clim. Past Discuss., https://doi.org/10.5194/cp-2018-138
Manuscript under review for journal Clim. Past
Discussion started: 5 November 2018
© Author(s) 2018. CC BY 4.0 License.

2 Data and Methods

2.1 Meteorological data

A daily gridded precipitation dataset for 1951-2007 was downloaded from APHRODITE (Asian Precipitation-Highly-Resolved Observational Data Integration Towards Evaluation of Water Resources, APHRO_MA_V1101R2 product, (21)) (Yatagai et al., 2009). The distributions of mean SPR (March-April) and EASM (May-September) precipitation amount in China from 1951 to 2007 are shown in Figure 1, which was exported based on this dataset by using the free software Ferret https://ferret.pmel.noaa.gov/Ferret/downloads.

Monthly precipitation datasets encompassing 160 meteorological stations in China during the period 1951-2014, which were obtained from National Climate Center (http://ncc.cma.gov.cn), were also used to characterize the percentage of spring (March-April) and EASM (May-September) precipitation amount relative to the annual precipitation amount over China.

Monthly mean $\delta^{18}O_p$ and precipitation amount data from meteorological stations over the MRC were obtained from the Global Network for Isotopes in Precipitation (GNIP) (http://www.iaea.org/) (Table 1 and Figure 1a). The monthly mean $\delta^{18}O_p$ data are used to compare the seasonal to interannual variation of $\delta^{18}O_p$ over the MRC. The stations near the coast from the southeastern region of the MRC (Fuzhou, Haikou, Hongkong, Guangzhou) were not used in this study because their precipitation amount and $\delta^{18}O_p$ are significantly influenced by typhoon in summer and autumn. Changsha station is the only one GNIP station in the SPR region.

2.2 $\delta^{18}O_p$ data from IsoGSM simulations

IsoGSM is a water isotope-incorporated general circulation model (Yoshimura et al., 2008). We use the product of IsoGSM nudged toward the NCEP/NCAR Reanalysis 2 (Kanamitsu et al., 2002) atmosphere and forced with observed sea surface temperatures (SST) and sea ice (Yoshimura et al., 2008). A detailed description of the model setup can be found in Yoshimura et al. (2008) and Yang et al. (2016). IsoGSM can reproduce reasonably well monthly variabilities of precipitation and water vapor isotopic compositions associated with synoptic weather cycles.

2.3 ENSO index

The ENSO plays an important role in governing the climatic variation over the MRC (e.g., Feng and Hu, 2004; Xue and Liu, 2008; Zhou and Chan, 2007). We used the multivariate ENSO Index (MEI), which is based on six oceanic-atmospheric variables (sea-level pressure, zonal and meridional components of the surface wind, SST and total cloudiness fraction of the sky) over the tropical Pacific, to examine the role of ENSO in influencing the rainfall over the MRC. The MEI is defined as the first principal component of above six variable fields, therefore, it provides a more complete description of

© Author(s) 2018. CC BY 4.0 License.

the ENSO phenomenon than a single variable ENSO index such as the Southern Oscillation Index (SOI) or Niño 3.4 SST (Wolter and Timlin, 2011). Positive and negative values of MEI represent El Niño and La Niña events, respectively. The data were obtained from the website of the Earth System Research Laboratory, National Oceanic & Atmospheric Administration (NOAA) (http://www.cdc.noaa.gov/people/klaus.wolter/MEI).

2.4 Back-trajectory analysis

MeteoInfo, which is a suite of software tools developed for meteorological data visualization and analysis, was used to perform air mass back trajectory calculations (Wang, 2014). The Hybrid Single-Particle Lagrangian Integrated Trajectory model (HYSPLIT) (Stein et al., 2015) is loaded into the MeteoInfo system as an external process (Wang et al., 2009). The parameter setting for trajectory calculation is similar to that in Cai et al. (2017). In order to get a qualitative view of the moisture source region and transport path for rainy season precipitation, only air mass back trajectories for precipitation-producing days were used. Trajectories were initiated four times daily (at UTC 00:00, 00:60, 12:00, and 18:00) during precipitating days (>1mm precipitation/day) and their air parcel was released at 1500 m above ground level and moved backward with winds for 240 hours (10 days). Multiple similar air mass trajectories were merged into clusters using the cluster analysis tool and the mean of each cluster were used to visualize the dominant trajectory paths.

3 Results

3.1 Proportions of SPR, EASM and NSM precipitation over MRC

We calculated the mean ratios of spring (March-April) to annual precipitation (spring/annual) and EASM (May-to-September) to annual precipitation (EASM/annual) ratios for the period 1951-2014. Figure 2a shows that the mean percentage of spring/annual in southeastern China (about 20 °N to 33 °N, 107 °E to 122 °E), which range from 10-25% and 0-10% in northern (about 33 °N to 53 °N, 100 °E to 134 °E) and southwestern regions of the MRC (about 20 °N to 33 °N, 90 °E to 107 °E), respectively. The Jiangxi and the eastern Hunan Provinces, the core regions of the SPR, show the highest mean percentage of spring/annual within the MRC (20-25%). which is consistent with the results from the previous studies (Tian and Yasunari, 1998; Wan and Wu, 2009). Figure 2b shows that the mean percentage of EASM/annual is 40-70% in southeastern China and 70-95% in other regions of the MRC. Conversely, the mean percentage of non-summer monsoon precipitation to annual precipitation (NSM/annual) is 30-60% in southeastern China and 5-30% in other regions of the MRC and reaches the maximum in the SPR region (45-60%). This indicates that the proportion of EASM precipitation (40-55%) is nearly equivalent to the proportion of NSM precipitation (45-60%) in the SPR region.

Clim. Past Discuss., https://doi.org/10.5194/cp-2018-138
Manuscript under review for journal Clim. Past
Discussion started: 5 November 2018
© Author(s) 2018. CC BY 4.0 License.

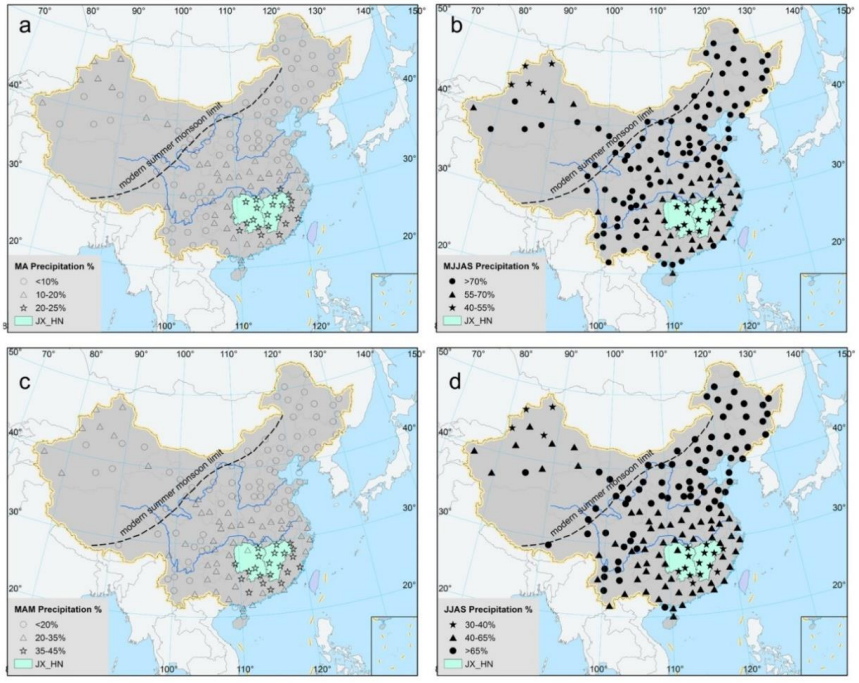

Figure 2. The percentage of spring (a, March to April) and EASM (b, May to September) precipitation amount relative to the annual precipitation amount over China. Figures c and d are similar to a and b, except that spring precipitation is shown from March to May in c and EASM precipitation between June and September in d. The Jiangxi and Hunan Provinces (JX_HN) are highlighted in jade color.

Usually, the SPR period lasts from March to mid-May (Wan and Wu, 2009) and the EASM period lasts from mid-May to September (Wang and Lin, 2002), however, the onset/retreat time of SPR and EASM and their intensities vary in different years (Zhou and Chan, 2007). The EASM starts late (late May to early June) and tends to be weaker during El Niño years (Huang et al., 2012) and EASM precipitation amount over Southeast China (SEC) is reduced when the SPR starts later (Wan et al., 2008a). Therefore, if we define the March-to-May precipitation as SPR and the June-to-September precipitation as EASM in El Niño years, the mean percentage of SPR/annual in the SPR region is 35-45% (Figure 2c), the mean percentage of EASM/annual is only 30-40% (Figure 2d), and the mean percentage of NSM/annual is 60-70%. However, in other regions of the MRC, the mean percentage of EASM/annual (65-90%) is still much higher than the mean percentage of NSM/annual (10-35%) (Figures 2c and d). Therefore, the distribution of EASM vs. NSM precipitation amount in SPR region is distinctly different from that in other regions of the MRC.

Clim. Past Discuss., https://doi.org/10.5194/cp-2018-138
Manuscript under review for journal Clim. Past
Discussion started: 5 November 2018
© Author(s) 2018. CC BY 4.0 License.

3.2 Seasonal precipitation amount and $\delta^{18}O_p$ over the MRC

We compared the seasonal variations of precipitation amount and $\delta^{18}O_p$ in the SPR region with those in other regions of the MRC by using data from the GNIP stations. According to the spatial distribution of EASM precipitation as discussed in section 3.1, we assigned Zhengzhou, Xi'an, Yantai, Shijiazhuang, and Tianjin GNIP stations to northern region of the MRC, Kunming, Guiyang, Zunyi, and Chengdu GNIP stations to southwestern region of the MRC, and Changsha, Guilin, Liuzhou, Nanjing, and Wuhan GNIP stations to southeastern China. Only the Changsha GNIP station is located in the SPR region (Table 1 and Figure 1a).

Table 1. GNIP stations used for the comparison of the seasonal precipitation amount and $\delta^{18}O_p$ over the MRC.

Category	Sites
Northern region of the MRC	Zhengzhou (34°43′12″N, 113°39′00″E)
	Xi'an (34°18′00″N, 108°55′48″E)
	Yantai (37°31′48″N, 121°24′00″E)
	Shijiazhuang (38°1′60″N, 114°25′01″E)
	Tianjin (39°6′00″N, 117°10′01″E)
Southwestern region of the MRC	Kunming (25°1′00″N, 102°40′59″E)
	Guiyang (26°34′60″N, 106°43′01″E)
	Zunyi (27°41′60″N, 106°52′48″E)
	Chengdu (30°40′12″N, 104°1′12″E)
Southeastern region of the MRC	Changsha (28°11′60″N, 113°4′01″E)
	Guilin (25°4′12″N, 110°4′48″E)
	Liuzhou (24°21′00″N, 109°24′00″E)
	Nanjing (32°10′48″N, 118°10′48″E)
	Wuhan (30°37′12″N, 114°7′48″E)

The seasonal variation of $\delta^{18}O_p$ over the MRC is consistently related to the onset, advancement, and retreat of the EASM. The $\delta^{18}O_p$ values decrease in May as the summer monsoon starts. The $\delta^{18}O_p$ values are relatively low during the monsoon season (June-August), because of the long-distance transport of water vapor from the distal Indian Ocean to the MRC. Along this pathway, progressive rainout leads to more negative $\delta^{18}O_p$ values via Rayleigh distillation (Baker et al., 2015; Liu et al., 2010; Rayleigh, 1896; Tan, 2014). The $\delta^{18}O_p$ values become progressively higher as the EASM withdraws in September. From October to next April, the $\delta^{18}O_p$ values are rather high, resulting from the short-distance transport of water vapor from the western Pacific Ocean or local moisture recycling (Wu

Clim. Past Discuss., https://doi.org/10.5194/cp-2018-138
Manuscript under review for journal Clim. Past
Discussion started: 5 November 2018
© Author(s) 2018. CC BY 4.0 License.

Climate of the Past Discussions
Open Access
EGU

et al., 2015; Tan et al., 2016). The low $\delta^{18}O_p$ values in winter in northern region of the MRC are caused by the temperature effect, but it is less important because of its small contribution to the amount-weighted mean annual precipitation $\delta^{18}O$ ($\delta^{18}O_w$) (Cheng et al., 2012). Therefore, the seasonal $\delta^{18}O_p$ values over the MRC show a broadly consistent pattern reaching a maximum in March-April and a minimum in July-August in the MRC with the exception of low winter $\delta^{18}O_p$ values in northern region of the MRC.

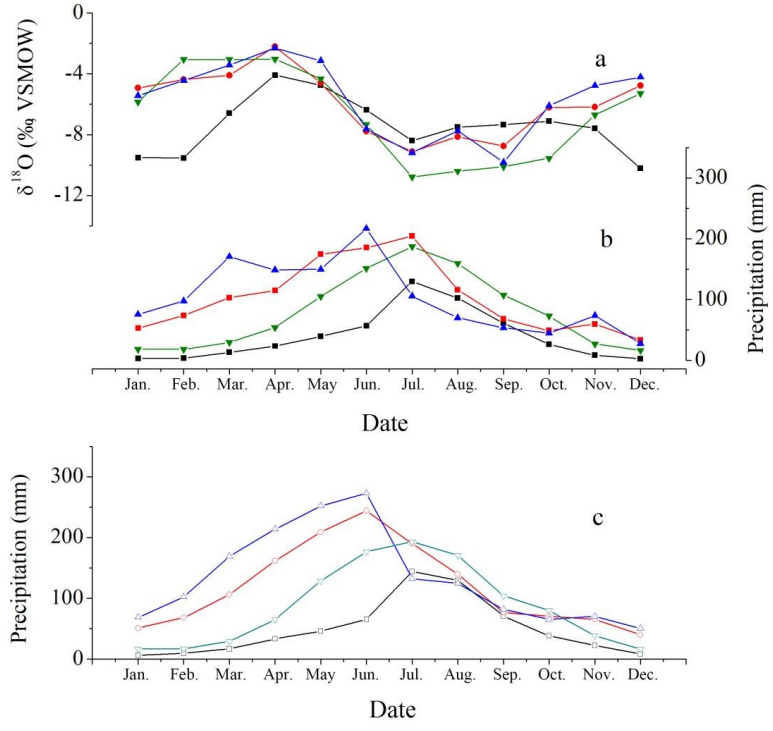

Figure 3. Monthly mean $\delta^{18}O_p$ (a) and precipitation amount (b) from GNIP stations in northern region of the MRC (black lines), southwestern region of the MRC (green lines), southeastern China (red lines), and the SPR region (blue lines, Changsha station) (see Table1 and Figure 1a). (c) Monthly mean precipitation amount from meteorological stations closest to the GNIP stations in northern region of the MRC (black lines), southwestern region of the MRC (jade lines), southeastern China (red lines), and the SPR region (blue lines).

Given that there are only a few years of data from those GNIP stations (Figure 3b), we obtained the mean monthly precipitation amount from the nearest meteorological stations in the MRC for the period 1951-2014 (Figure 3c). Both datasets show that the seasonal variation of precipitation amount in southeastern China, especially in the SPR region, is different from that in other regions of the MRC (Figures 3b and c). The precipitation amount in March and April before the onset of EASM is high

Clim. Past Discuss., https://doi.org/10.5194/cp-2018-138
Manuscript under review for journal Clim. Past
Discussion started: 5 November 2018
© Author(s) 2018. CC BY 4.0 License.

Climate of the Past Discussions
Open Access
EGU

over SEC. It is even higher than the summer monsoon precipitation amount in June, July and August in other regions of the MRC. In the SPR region, the summer monsoon rainfall amount in July-August is much smaller than the rainfall in March-April. However, in other regions of the MRC, the summer monsoon rainfall in July-August is the highest of the whole year.

3.3 Air mass back trajectory

The trajectories for GNIP Changsha station during EASM and NSM seasons were identified in a La Niña phase (1988-1989) with low-$\delta^{18}O_p$ anomalies and in an El Niño phase (1991-1992) with high -$\delta^{18}O_p$ anomalies, respectively (Figure 4). It shows that the air mass trajectories and origins during EASM season are different between El Niño and La Niña phases as well as those during NSM season. During EASM season, three categories of trajectories are identified with 30.4% moisture originating from North China, 33.9% from South China Sea, and 35.7% from remote Indian Ocean in the La Niña phase (Figure 4a). In the El Niño phase, the moisture sources originate from western Pacific (46.1%) and Indian Ocean (45.1%) (Figure 4c). In previous studies, researchers mainly focus on the variations in moisture source during EASM season (Baker et al., 2015; Cai et al., 2017; Tan, 2014), however, we also analyzed the back-trajectories during NSM season because the NSM precipitation contributing ~50% to the annual precipitation in the SPR region. It shows that less moisture (30%, C2 in Figure 4b) originates from western Pacific but more moisture (35.3%, C3 in Figure 4b) from Indochina Peninsula in the La Niña phase than those in the El Niño phase (Figure 4d). The effect of moisture source on the $\delta^{18}O_p$ variation will be discussed in next section 4.1.

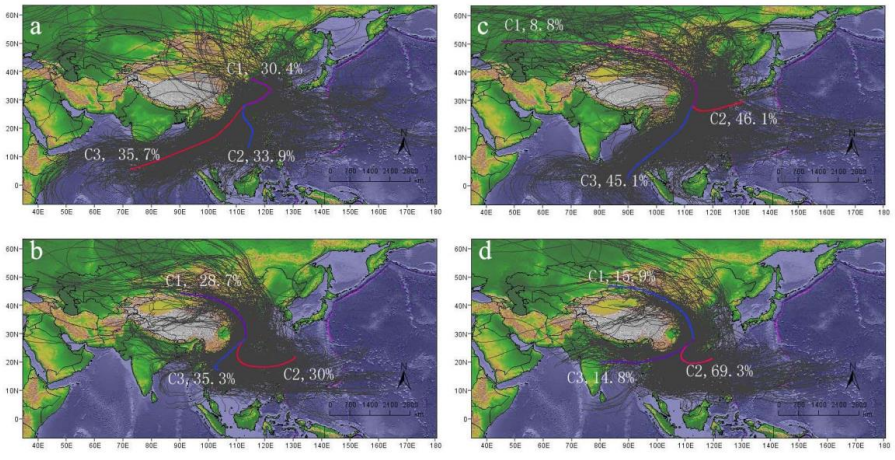

Figure 4. Cluster means of precipitation-producing back trajectories starting at Changsha station during EASM and NSM seasons in El Niño and La Niña phases, respectively. (a) and (b) show the air mass trajectories and origins during EASM and NSM seasons in a La Niña phase (1988-1989),

Clim. Past Discuss., https://doi.org/10.5194/cp-2018-138
Manuscript under review for journal Clim. Past
Discussion started: 5 November 2018
© Author(s) 2018. CC BY 4.0 License.

235 respectively; (c) and (d) are the same as (a) and (b) but in an El Niño phase (1991-1992). Multiple similar air mass trajectories (grey lines) were merged into clusters using the cluster analysis tool and the mean of each cluster were used to visualize the dominant trajectory paths.

4 Discussion

4.1 Amount-weighted mean annual precipitation $\delta^{18}O$

240 In principle, the amount-weighted mean annual precipitation $\delta^{18}O$ ($\delta^{18}O_w$) should be calculated as the following:

$$\delta^{18}O_w=(P_{Jan}\times\delta^{18}O_{Jan}+P_{Feb}\times\delta^{18}O_{Feb}+\ldots\ldots P_{Dec}\times\delta^{18}O_{Dec})/(P_{Jan}+P_{Feb}+\ldots\ldots P_{Dec}) \quad \text{Eq. (1)}$$

Based on the characteristics of the precipitation amount and $\delta^{18}O$ during EASM and NSM seasons over the MRC, the equation above can be written in the following mode:

245 $$\delta^{18}O_w \approx (P_{EASM\text{-}mean}\times\delta^{18}O_{EASM\text{-}mean}+P_{NSM\text{-}mean}\times\delta^{18}O_{NSM\text{-}mean})/(P_{EASM\text{-}mean}+P_{NSM\text{-}mean})$$

$$=EASM\%\times\delta^{18}O_{EASM\text{-}mean}+NSM\%\times\delta^{18}O_{NSM\text{-}mean} \quad \text{Eq. (2)}$$

where $P_{EASM\text{-}mean}$ and $P_{NSM\text{-}mean}$ indicate the mean precipitation amount of EASM and NSM, $\delta^{18}O_{EASM\text{-}mean}$ and $\delta^{18}O_{NSM\text{-}mean}$ indicate the mean value of EASM and NSM precipitation, EASM% and NSM% indicate the mean percentage of the EASM precipitation amount, respectively.

250 Therefore, we can consider that the $\delta^{18}O_w$ is controlled by both rainfall amount and $\delta^{18}O_p$ values during EASM and NSM season over MRC. Given the relationship between monthly precipitation amount and $\delta^{18}O_p$ over MRC (Figure 3), we can find that: 1) In northern and southwestern regions of the MRC, $\delta^{18}O_w$ are mainly controlled by the amount and $\delta^{18}O$ of EASM precipitation because the precipitation amount of the EASM with rather low $\delta^{18}O_p$ values accounts for 70% of the annual 255 precipitation and the NSM precipitation is only a small contribution to the $\delta^{18}O_w$ (less than 30%); 2) Over SEC, especially in the SPR region, the precipitation amount of the NSM with rather high $\delta^{18}O_p$ values even exceeds that of the EASM with rather low $\delta^{18}O_p$ values, and it also has an important effect on $\delta^{18}O_w$. Hence, $\delta^{18}O_w$ in the SPR region is affected by both EASM and NSM precipitation. In addition, except the effect of the seasonal distribution of precipitation amount, the seasonal $\delta^{18}O$ itself 260 also attributes to the $\delta^{18}O_w$, which is related to the variations in moisture sources, pathways, and so on (Baker et al., 2015; Huang et al., 2017; Tan et al., 2016).

Tan (2014) suggested that positive (negative) $\delta^{18}O_w$ anomalies during El Niño (La Niña) phases reflect more (less) water vapor originating from the nearby South China Sea and the Western Pacific Ocean (characterized by rather high $\delta^{18}O_p$ values) relative to the remote Indian Ocean (showing rather 265 low $\delta^{18}O_p$ values). Using a Lagrangian precipitation moisture source diagnostic, however, Baker et al. (2015) suggested that EASM precipitation is primarily derived from the Indian Ocean, Pacific Ocean

Clim. Past Discuss., https://doi.org/10.5194/cp-2018-138
Manuscript under review for journal Clim. Past
Discussion started: 5 November 2018
© Author(s) 2018. CC BY 4.0 License.

moisture export peaks during winter, and the moisture uptake area does not differ significantly between summer and winter; changes in moisture transport may impact the $\delta^{18}O$ variation of EASM precipitation. By using the Hybrid Single-Particle Lagrangian Integrated Trajectory (HYSPLIT) model, Cai et al. (2017) also demonstrated that the moisture sources vary little between years with relatively high and low $\delta^{18}O$ values (corresponding to El Niño and La Niña years) in the EASM region, the EASM rainfall is primarily derived from the Indian Ocean, while the Pacific Ocean moisture is a minor contributor. Only trajectories delivering precipitation to the target regions were considered in these two studies. Dayem et al. (2010) proposed that several processes (e.g., different source regions, pathways and types of precipitation) contribute to the $\delta^{18}O_p$ variation. In section 3.3, we also analyzed the variations in moisture source between El Niño and La Niña phases. During EASM season, 64.3% moisture originating from North China and South China Sea (C1 and C2 in Figure 4a) in La Niña phase and 54.9% moisture originating from western Pacific and Westerlies (C1 and C2 in Figure 4c) in El Niño phase. There are only ~9% difference of the moisture originating from Indian Ocean characterized by relatively low $\delta^{18}O_p$ values (C3 in Figure 4a and 4c) between El Niño and La Niña phases, which is consistent with the results in Baker et al. (2015) and Cai et al. (2017). Therefore, we suggest that the variation in moisture source during EASM period, in some extent, might contribute to the changes in $\delta^{18}O_w$, but it should not be the key factor. Apart from the possible factors of moisture source during EASM season, however, we also emphasize the effect of precipitation in NSM season on $\delta^{18}O_w$ in the SPR region. During NSM season, the moistures originating from Westerlies, western Pacific and Indochina Peninsula are characterized by relatively high $\delta^{18}O_p$ values, the variations in moisture source between El Niño and La Niña phases should not be the key factor influencing the variations in $\delta^{18}O_w$ value, either. Therefore, we try to analysis the relationship between the seasonal precipitation amount and $\delta^{18}O_w$ with ENSO on interannual timescale in the next section.

4.2 Interannual variation of precipitation amount and $\delta^{18}O_w$ over the SPR region influenced by ENSO

The ENSO is a coupled oceanic-atmospheric phenomenon controlling the interannual variation in precipitation amount and $\delta^{18}O$ over southeastern China (e.g., Feng and Hu, 2004; Huang et al., 2017; Tan et al., 2014; Xue and Liu, 2008; Yang et al., 2016). Our analysis of the 1988-1992 data from the Changsha GNIP station suggest that the mean value of $\delta^{18}O_w$ (-6.73‰) in La Niña years (1988-1989) is significantly more negative than that during the El Niño years (1991-1992; -4.11‰). However, there is no significant variation in the annual precipitation amount between La Niña and El Niño years (Figure 5a). The differences of $\delta^{18}O_w$ between La Niña and El Niño phases cannot be explained by the variations in annual precipitation amount. This is consistent with the analyses based on instrumental meteorological data (Huang et al., 2017; Tan, 2014) and climate simulations (Yang et al., 2016). Indeed, there is more summer monsoon precipitation in June-to-September during La Niña years (1988-1989)

Clim. Past Discuss., https://doi.org/10.5194/cp-2018-138
Manuscript under review for journal Clim. Past
Discussion started: 5 November 2018
© Author(s) 2018. CC BY 4.0 License.

but more SPR in March-April during El Niño years (1991-1992), though the annual precipitation amount is similar (Figure 5b). We find that the $\delta^{18}O_w$ variability is broadly consistent with the variation in the ratio of EASM/NSM precipitation amount during 1988-1992 (Figure 5). Unfortunately, the data series from the Changsha GNIP station is too short (5 years) to evaluate the relationship between the EASM/NSM ratio and $\delta^{18}O_p$ in the SPR region. Therefore, we used the average precipitation data from 11 meteorological stations (1951-2014) in the Jiangxi Province and the eastern Hunan Province (i.e. from the core area of the SPR) and the $\delta^{18}O$ data obtained from IsoGSM simulation (1979-2009), to examine the relationship between ENSO, $\delta^{18}O_w$ and precipitation amount in the SPR region on interannual timescales.

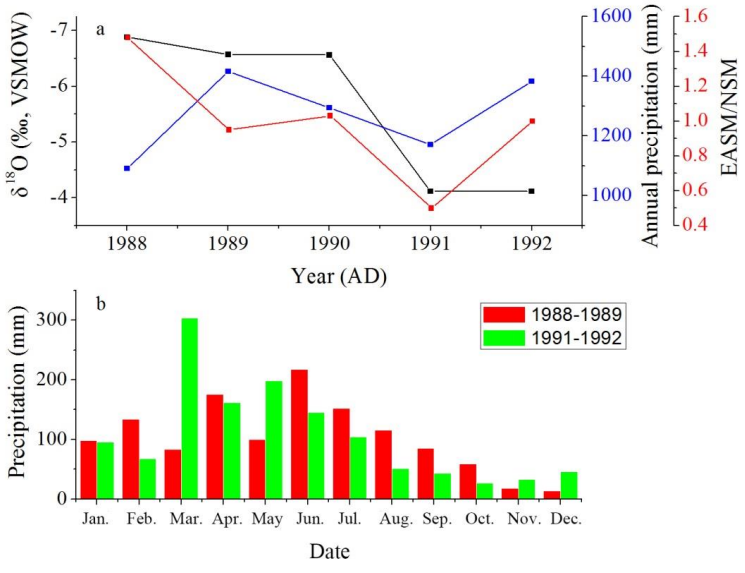

Figure 5. Comparisons between ENSO events, precipitation amount and $\delta^{18}O_w$ at the Changsha GNIP station for the period 1988-1992. (a) Comparison between annual precipitation amount, $\delta^{18}O_w$, and the EASM/NSM ratio. (b) Comparison of mean monthly precipitation amount between La Niña (1988-1989) and El Niño (1991-1992) years.

We calculated correlation coefficients among the $\delta^{18}O_w$, MEI, the EASM/NSM ratio, and the annual, EASM, and NSM precipitation amount for 1979-2009 (Table 2 and Figure 6). The results show that the time series of the simulated $\delta^{18}O_w$ data significantly correlates with the MEI (r=0.52, $p<0.01$), consistent with the positive relationship between the ENSO index and $\delta^{18}O_w$ observed in modern precipitation (Huang et al., 2017; Tan, 2014; Yang et al., 2016) as well as in the $\delta^{18}O$ records of speleothems and tree-ring cellulose (Tan, 2016; Xu et al., 2013, 2016a, 2016b; Zhang et al., 2018), and

Clim. Past Discuss., https://doi.org/10.5194/cp-2018-138
Manuscript under review for journal Clim. Past
Discussion started: 5 November 2018
© Author(s) 2018. CC BY 4.0 License.

Climate of the Past Discussions

furthermore, the same relationship holds for the Changsha GNIP station (Figure 5a). It indicates that the precipitation $\delta^{18}O_w$ is higher (lower) in El Niño (La Niña) phase in the SPR region. The time series of the simulated $\delta^{18}O_w$ data significantly correlates with the EASM precipitation amount (r=-0.39, *p<0.05*) and the EASM/NSM ratio (r=-0.45, *p<0.05*) (Table 2). The 1yr-lag time series of the simulated $\delta^{18}O_w$ data also significantly correlates with the EASM precipitation amount (r=-0.44, *p<0.01*) and the EASM/NSM ratio (r=-0.53, *p<0.01*) (Table 2 and Figure 6). There is, however, no significant correlation between the $\delta^{18}O_w$ and the annual precipitation amount, consistent with the result based on instrumental data from Changsha station (Figure 5a) and other studies (Tan et al., 2014; Yang et al., 2016).

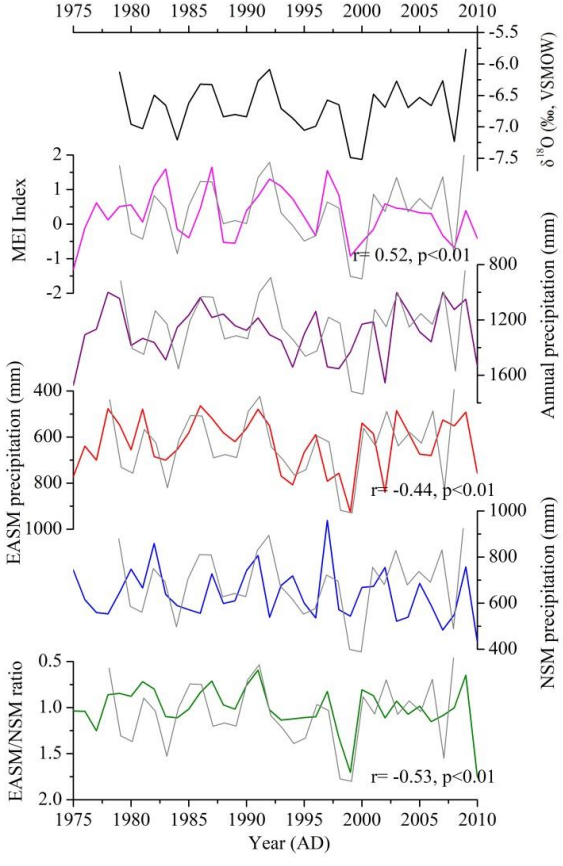

Figure 6. Correlations between the time series of the $\delta^{18}O_w$ (black line), MEI (pink line), the annual (purple line), EASM (red line) and NSM (blue line) precipitation amount, and the EASM/NSM ratio (green line) in the SPR region during 1979-2009. The time series of the $\delta^{18}O_w$ lags the time series of EASM precipitation amount and the EASM/NSM ratio by 1 yr.

Clim. Past Discuss., https://doi.org/10.5194/cp-2018-138
Manuscript under review for journal Clim. Past
Discussion started: 5 November 2018
© Author(s) 2018. CC BY 4.0 License.

Table 2. Correlation coefficients between the time series of the $\delta^{18}O_w$, MEI, the EASM/NSM ratio, and the annual, EASM, and NSM precipitation amount in the SPR region for 1979-2009. * indicates significant correlation at the 0.05 level (2-tailed). ** indicates significant correlation at the 0.01 level (2-tailed).

	MEI	Anuall rainfall amount	EASM rainfall amount	NSM rainfall amount	EASM/NSM ratio
$\delta^{18}O_w$	0.52**	-0.34	-0.39*	0.16	-0.45*
1 yr lag $\delta^{18}O_w$		-0.27	-0.44**	0.15	-0.53**

In order to find out the relationship between ENSO and the seasonal precipitation amount, we also calculated correlation coefficients between the multivariate ENSO Index (MEI), the EASM/NSM ratio, and the annual, EASM, and NSM precipitation amount for 1951-2014 (Table 3). The mean value of October-next June MEI significantly correlates with the EASM precipitation amount (r=-0.28, *p<0.05*), NSM precipitation amount (r=0.52, *p<0.01*) and the EASM/NSM ratio (r=-0.53, *p<0.05*) (Table 3). It indicates that, on interannual timescales, there are decreased EASM precipitation during the developing stage of El Niño and increased NSM precipitation during the mature stage of El Niño, resulting in lower EASM/NSM ratios during El Niño phases; and vice versa. There is, however, no significant correlation between the MEI and the annual precipitation amount. In addition, the EASM/NSM ratio significantly correlates with the EASM (r=0.74, *p<0.01*) and the NSM (r=-0.46, *p<0.01*) (Table 3).

Previous studies found that decreased summer rainfall in the south of Yangtze River occurs during the developing stage of El Niño, resulting from southward shift of the subtropical high associated with colder SST in the western tropical Pacific and weak convective activities around South China Sea and the Philippines (Huang and Wu, 1989; Zhang et al., 1999). Kong and Tu (2003) also found that there is less EASM rainfall in May-September in the lower reaches of Yangtze River valley during 14 El Niño events since 1950s. The same relationship is observed in the May-October rainfall reconstruction based on tree ring cellulose $\delta^{18}O$ (Xu et al., 2016a), during El Niño phases, colder summer SST in western Pacific leading to weakened western Pacific Subtropical High results in less rainfall during May-October in the middle-lower valleys of Yangtze River (Liu and Li, 2011; Xu et al., 2016a), and vice versa. Meanwhile, increased rainfall in the autumn, winter and spring (i.e. NSM) can be found in southern China during the mature stage of El Niño (Wan et al., 2008b; Wang et al. 2000; Zhang et al., 1999; Zhang et al., 2015; Zhou, 2011; Zhou and Wu, 2010). During the El Niño mature phases, lower-level southwesterly anomalies over South China Sea transports more moisture into SEC, leading to increased NSM precipitation (Wang et al., 2000; Zhang et al., 1999; Zhou, 2011; Zhou and Wu, 2010). These conclusions are consistent with our finding in the SPR region. It is notable that the there is no significant variations in EASM precipitation amount in our study area during the decaying stage

Clim. Past Discuss., https://doi.org/10.5194/cp-2018-138
Manuscript under review for journal Clim. Past
Discussion started: 5 November 2018
© Author(s) 2018. CC BY 4.0 License.

of El Niño, although increased summer rainfall was observed in southern China in previous studies (Huang and Wu, 1989).

Given the relationship between the $\delta^{18}O_w$, MEI, and seasonal precipitation amount, we can find that less (more) EASM and more (less) NSM precipitation lead to lower (higher) EASM/NSM ratios resulting in higher (lower) $\delta^{18}O_w$ values in the SPR region during El Niño (La Niña) phases. We therefore suggest that, over the SPR region, the precipitation seasonality (i.e., the EASM/NSM ratio) modulated by ENSO plays a key role in governing the interannual variability of $\delta^{18}O_w$, although moisture sources and pathways may also play a role (Baker et al., 2015; Huang et al., 2017; Tan et al., 2016).

Table 3. Correlation coefficients between the time series of the MEI, the EASM/NSM ratio, and the annual, EASM, and NSM precipitation amount in the SPR region for 1951-2014. * indicates significant correlation at the 0.05 level (2-tailed). ** indicates significant correlation at the 0.01 level (2-tailed).

	Anuall rainfall amount	EASM rainfall amount	NSM rainfall amount	EASM/NSM ratio
MEI (Oct-next Jun)	-0.13	-0.28*	0.52**	-0.53**
Anuall rainfall amount		0.84**	0.22	0.47**
EASM rainfall amount			-0.01	0.74**
NSM rainfall amount				-0.65**

4.3 Implication for paleoclimatic reconstructions

Although $\delta^{18}O_s$ records have significantly improved our understanding of the EASM variability on different timescales, the significance and quantification of these proxy records is still a subject of debate because $\delta^{18}O_s$ is influenced by several competing factors. We emphasize that the spatial differences in seasonal precipitation over the MRC are key to understand the $\delta^{18}O_s$-climate relationship. Figure 1 illustrates that (1) Wanxiang (Zhang et al., 2008), Dayu (Tan et al., 2009), Huangye (Tan et al., 2010), Wuya (Tan et al., 2014), Shihua (Li et al., 2017), and Xiaobailong (Tan et al., 2017) caves are located in northern and southwestern regions of the MRC, where $\delta^{18}O_w$ is primarily controlled by the EASM/annual precipitation amount. Therefore, these records show a significant correlation with the instrumental precipitation or the regional drought/flood (D/F) index obtained from historical documents (e.g., Li et al., 2017; Liu et al., 2008; Tan et al., 2009, 2010, 2014, 2017; Zhang et al., 2008). (2) Dongge (Yuan et al., 2004), Heshang (Hu et al., 2008), Hulu (Wang et al., 2001), Yuhua (Jiang et al., 2012) and E'mei (Zhang et al., 2018) caves are located in southeastern China, where $\delta^{18}O_w$ is not only affected by EASM precipitation but also by NSM precipitation. Hence, according to Wang et al. (2001) $\delta^{18}O_s$ from Hulu cave reflects the ratio of summer to winter precipitation amount. Factors related to the

Clim. Past Discuss., https://doi.org/10.5194/cp-2018-138
Manuscript under review for journal Clim. Past
Discussion started: 5 November 2018
© Author(s) 2018. CC BY 4.0 License.

NSM (e.g., moisture source, precipitation seasonality, winter temperature) have also been taken into consideration in the interpretation of $\delta^{18}O_s$ in southeastern China (e.g., Baker et al., 2015; Clemens et al., 2010; Dayem et al., 2010; Zhang et al., 2018). On the other hand, the high percentage of NSM precipitation with relatively high $\delta^{18}O_p$ values in southeastern China should be an important reason why $\delta^{18}O_w$ and $\delta^{18}O_s$ are much lower and their variability is much larger in southwestern China than in southeastern China (Li et al., 2016; Liu et al., 2010; Zhang et al., 2018), except for the influence of moisture sources and pathways during the EASM season.

We find that the precipitation seasonality modulated by ENSO mainly controls the $\delta^{18}O_w$ values in the SPR region, with lower (higher) EASM/NSM ratios associated with El Niño (La Niña) phases resulting in higher (lower) $\delta^{18}O_w$ values. Therefore, we suggest that the interannual variability of $\delta^{18}O_s$ in the SPR region is primarily controlled by precipitation seasonality (i.e., the EASM/NSM ratio) modulated by ENSO, although changes in moisture sources and pathways may also play a role (Baker et al., 2015; Dayem et al., 2010; Maher, 2008, 2016; Tan, 2016). In addition, the ENSO index also significantly correlates with the EASM precipitation amount in the SPR region, implying that additional studies are needed to disentangle the main driving factor (e.g., EASM precipitation amount vs. EASM/NSM ratio) operating on different timescales. Few $\delta^{18}O_s$ records have been published for the SPR region so far (Jiang et al., 2012; Zhang et al., 2018). Such long-term records, however, are critically needed to examine the climate-proxy relationship both on interannual and on decadal to millennial timescales.

5 Conclusions

We find that the distribution of seasonal precipitation amount in southeastern China, especially in the SPR region, is different from other regions of the MRC for the time interval of this study (1951-2014 AD). In the SPR region, the mean precipitation amount of EASM is equivalent to that of NSM. However, in northern and southwestern regions of the MRC, the mean percentage of EASM to the annual precipitation amount exceeds 70%. The seasonal $\delta^{18}O_p$ over the MRC shows broadly consistent variations with relatively low and high values for EASM and NSM precipitation, respectively. The low $\delta^{18}O_p$ values associated with winter precipitation in northern region of the MRC, however, is only a minor contribution to $\delta^{18}O_w$. Thus, the NSM precipitation in the SPR region also has an important effect on $\delta^{18}O_w$, but the $\delta^{18}O_w$ in northern and southwestern regions is primarily influenced by EASM precipitation.

Based on a statistical analysis of the ENSO index, simulated $\delta^{18}O$ data and seasonal precipitation amount in the SPR region, we find less (more) EASM and more (less) NSM precipitation lead to a lower (higher) EASM/NSM ratio that results in higher (lower) $\delta^{18}O_w$ in the SPR region during El Niño (La Niña) phases. Recognizing this spatial difference in seasonal precipitation is therefore, important in

© Author(s) 2018. CC BY 4.0 License.

understanding the robust significance of $\delta^{18}O_s$ in the MRC. On interannual timescales, the $\delta^{18}O_s$ variability in northern and southwestern regions of the MRC is primarily influenced by the EASM or the annual precipitation amount; in the SPR region, however, precipitation seasonality (i.e., the EASM/NSM ratio) modulated by ENSO plays a key role in governing $\delta^{18}O_s$ variability, although moisture source and pathways may also play a role.

6 Author Contributions

H.W.Z designed the research and wrote the first draft of the manuscript. H.C. Y.J.C. C.S. and A.S. revised the manuscript. All authors discussed the results and provided input on the manuscript.

7 Competing interests

The authors declare no competing interests.

Acknowledgments

Thanks to Ming Tan for reviewing the manuscript and giving many constructive suggestions. Thanks to Hui Tang, Zhongyin Cai and Hanyin Li for helping to do the back-trajectory analyses. This study was supported by the NSFC (41502166), the China Postdoctoral Science Foundation (2015M580832), the State Key Laboratory of Loess and Quaternary Geology (SKLLQG1046) and the Key Laboratory of Karst Dynamics, Ministry of Land and Resources of the People's Republic of China (MLR) and GZAR (KDL201502).

References

Baker, A. J., Sodemann, H., Baldini, J. U., Breitenbach, S. F., Johnson, K. R., Hunen, J., and Zhang, P.: Seasonality of westerly moisture transport in the East Asian summer monsoon and its implications for interpreting precipitation $\delta^{18}O$, Journal of Geophysical Research: Atmospheres, 120, 5850-5862, 2015.

Cai, Y., Fung, I. Y., Edwards, R. L., An, Z., Cheng, H., Lee, J.-E., Tan, L., Shen, C.-C., Wang, X., and Day, J. A.: Variability of stalagmite-inferred Indian monsoon precipitation over the past 252,000 y, Proceedings of the National Academy of Sciences, 112, 2954-2959, 2015.

Cai, Z., Tian, L., and Bowen, G. J.: ENSO variability reflected in precipitation oxygen isotopes across the Asian Summer Monsoon region, Earth and Planetary Science Letters, 475, 25-33, 2017.

Caley, T., Roche, D. M., and Renssen, H.: Orbital Asian summer monsoon dynamics revealed using an isotope-enabled global climate model, Nature communications, 5, 5371, 2014.

Cheng, H., Edwards, R. L., Broecker, W. S., Denton, G. H., Kong, X., Wang, Y., Zhang, R., and Wang, X.: Ice age terminations, Science, 326, 248-252, 2009.

© Author(s) 2018. CC BY 4.0 License.

Cheng, H., Edwards, R. L., Sinha, A., Spötl, C., Yi, L., Chen, S., Kelly, M., Kathayat, G., Wang, X., Li, X., Kong, X., Wang, Y., Ning, Y., and Zhang, H.: The Asian monsoon over the past 640,000 years and ice age terminations, Nature, 534, 640-646, 2016.

Cheng, H., Sinha, A., Wang, X., Cruz, F. W., and Edwards, R. L.: The Global Paleomonsoon as seen through speleothem records from Asia and the Americas, Climate Dynamics, 39, 1045-1062, 2012.

Clemens, S. C., Prell, W. L., and Sun, Y.: Orbital‐scale timing and mechanisms driving Late Pleistocene Indo-Asian summer monsoons: Reinterpreting cave speleothem $\delta^{18}O$, Paleoceanography, 25, PA4207, 2010.

Dayem, K. E., Molnar, P., Battisti, D. S., and Roe, G. H.: Lessons learned from oxygen isotopes in modern precipitation applied to interpretation of speleothem records of paleoclimate from eastern Asia, Earth and Planetary Science Letters, 295, 219-230, 2010.

Ding, Y., Chen, L., and Murakami, M.: The East Asian Monsoon [M]. Beijing: China Meteorological Press, 1994.

Ding, Y.: Summer monsoon rainfalls in China, Journal of the Meteorological Society of Japan. Ser. II, 70, 373-396, 1992.

Feng, J. and Li, J.: Influence of El Niño Modoki on spring rainfall over south China, Journal of Geophysical Research: Atmospheres, 116, D13102, 2011.

Feng, S. and Hu, Q.: Variations in the teleconnection of ENSO and summer rainfall in northern China: a role of the Indian summer monsoon, Journal of Climate, 17, 4871-4881, 2004.

He, J., Zhao, P., Zhu, C., Zhang, R., Tang, X., Chen, L., and Zhou, X.: Discussion of some problems as to the East Asian subtropical monsoon, Journal of Meteorological Research, 22, 419-434, 2008.

Hu, C., Henderson, G., Huang, J., Xie, S., Sun, Y., and Johnson, K.: Quantification of Holocene Asian monsoon rainfall from spatially separated cave records, Earth and Planetary Science Letters, 266, 221-232, 2008.

Huang, R. and Wu, Y.: The influence of ENSO on the summer climate change in China and its mechanism, Advances in Atmospheric Sciences, 6, 21-32, 1989.

Huang, R., Chen, J., Wang, L., and Lin, Z.: Characteristics, processes, and causes of the spatio-temporal variabilities of the East Asian monsoon system, Advances in Atmospheric Sciences, 29, 910-942, 2012.

Huang, Y., Song, X., Zhang, X., He, Q., Han, Q., and Li, Q.: Relationship of Stable Water Isotopes in Precipitation with ENSO in Dongting Lake Basin, Scientia Geographica Sinica 37, 792-798, 2017. (In Chinese with English abstract)

Jiang, X. Y., Li, Z. D., Li, J. Q., Kong, X. G., and Guo Y.: Stalagmite $\delta^{18}O$ record from Yuhua cave over the past 500 years and its regional climate significance, Scientia Geographica Sinica, 32: 207-212, 2012. (In Chinese with English abstract)

Kanamitsu, M., Ebisuzaki, W., Woollen, J., Yang, S.-K., Hnilo, J., Fiorino, M., and Potter, G.: Ncep–doe amip-ii reanalysis (r-2), Bulletin of the American Meteorological Society, 83, 1631-1644, 2002.

© Author(s) 2018. CC BY 4.0 License.

Kong, C. Y. and Tu, Q. P.: Influence of El Niño events on summer precipitation in east China under different climatic backgrounds, Journal of Nanjing Institute of Meteorology, 1, 84-88, 2003. (In Chinese with English abstract)

Li, X., Cheng, H., Tan, L., Ban, F., Sinha, A., Duan, W., Li, H., Zhang, H., Ning, Y., and Kathayat, G.: The East Asian summer monsoon variability over the last 145 years inferred from the Shihua Cave record, North China, Scientific reports, 7, 7078, 2017.

Li, Y., Rao, Z., Cao, J., Jiang, H., and Gao, Y.: Highly negative oxygen isotopes in precipitation in southwest China and their significance in paleoclimatic studies, Quaternary International, 2016. 2016.

Liu, J., Song, X., Yuan, G., Sun, X., Liu, X., and Wang, S.: Characteristics of $\delta^{18}O$ in precipitation over Eastern Monsoon China and the water vapor sources, Chinese Science Bulletin, 55, 200-211, 2010.

Liu, J., Zhang, P., Cheng, H., Chen, F., Yang, X., Zhang, D., Zhou, J., Jia, J., An, C., and Sang, W.: Asian summer monsoon precipitation recorded by stalagmite oxygen isotopic composition in the western Loess Plateau during AD1875–2003 and its linkage with ocean-atmosphere system, Chinese Science Bulletin, 53, 2041-2049, 2008.

Liu, N. and Li, Z.: Relationship of the western Pacific warm pool SST anomaly and summer precipitation in China, Meteorology & Disaster Reduction Research, 34, 8-13, 2011. (In Chinese with English abstract)

Maher, B. A. and Thompson, R.: Oxygen isotopes from Chinese caves: records not of monsoon rainfall but of circulation regime, Journal of Quaternary Science, 27, 615-624, 2012.

Maher, B. A.: Holocene variability of the East Asian summer monsoon from Chinese cave records: a re-assessment, The Holocene, 18, 861-866, 2008.

Maher, B. A.: Palaeoclimatic records of the loess/palaeosol sequences of the Chinese Loess Plateau, Quaternary Science Reviews, 154, 23-84, 2016.

Pausata, F. S., Battisti, D. S., Nisancioglu, K. H., and Bitz, C. M.: Chinese stalagmite $\delta^{18}O$ controlled by changes in the Indian monsoon during a simulated Heinrich event, Nature Geoscience, 4, 474-480, 2011.

Rayleigh, L.: L. Theoretical considerations respecting the separation of gases by diffusion and similar processes, The London, Edinburgh, and Dublin Philosophical Magazine and Journal of Science, 42, 493-498, 1896.

Stein, A., Draxler, R. R., Rolph, G. D., Stunder, B. J., Cohen, M., and Ngan, F.: NOAA's HYSPLIT atmospheric transport and dispersion modeling system, Bulletin of the American Meteorological Society, 96, 2059-2077, 2015.

Tan, L., An, Z., Huh, C.-A., Cai, Y., Shen, C.-C., Shiau, L.-J., Yan, L., Cheng, H., and Edwards, R. L.: Cyclic precipitation variation on the western Loess Plateau of China during the past four centuries, Scientific reports, 4, 6381, 2014.

© Author(s) 2018. CC BY 4.0 License.

Tan, L., Cai, Y., An, Z., Cheng, H., Shen, C.-C., Gao, Y., and Edwards, R. L.: Decreasing monsoon precipitation in southwest China during the last 240 years associated with the warming of tropical ocean, Climate Dynamics, 48, 1769-1778, 2017.

Tan, L., Cai, Y., An, Z., Edwards, R. L., Cheng, H., Shen, C. C., and Zhang, H.: Centennial-to decadal-scale monsoon precipitation variability in the semi-humid region, northern China during the last 1860 years: Records from stalagmites in Huangye Cave, The Holocene, 21, 287-296, 2010.

Tan, L., Cai, Y., Cheng, H., An, Z., and Edwards, R. L.: Summer monsoon precipitation variations in central China over the past 750 years derived from a high-resolution absolute-dated stalagmite, Palaeogeography, Palaeoclimatology, Palaeoecology, 280, 432-439, 2009.

Tan, M., Nan, S., and Duan, W.: Seasonal scale circulation effect of stable isotope in atmospheric precipitation in the monsoon regions of China, Quaternary Research, 36, 575-580, 2016. (In Chinese with English abstract)

Tan, M.: Circulation background of climate patterns in the past millennium: Uncertainty analysis and re-reconstruction of ENSO-like state, Science China Earth Sciences, 59, 1225-1241, 2016.

Tan, M.: Circulation effect: response of precipitation $\delta^{18}O$ to the ENSO cycle in monsoon regions of China, Climate Dynamics, 42, 1067-1077, 2014.

Tian, S.-F. and Yasunari, T.: Climatological aspects and mechanism of spring persistent rains over central China, Journal of the Meteorological Society of Japan. Ser. II, 76, 57-71, 1998.

Wan, R. and Wu, G.: Mechanism of the spring persistent rains over southeastern China, SCIENCE IN China Series D: Earth Sciences, 50, 130-144, 2007.

Wan, R. and Wu, G.: Temporal and spatial distributions of the spring persistent rains over Southeastern China, Journal of Meteorological Research, 23, 598-608, 2009.

Wan, R., Wang, T., and Wu, G.: Temporal variations of the spring persistent rains and South China Sea sub-high and their correlations to the circulation and precipitation of the East Asian Summer Monsoon, Journal of Meteorological Research, 22, 530-537, 2008a.

Wan, R., Zhao, B. K., and Hou, Y. L.: Interannual variability of spring persistent rain over southeastern China and its effect factor, Plateau Meteorology, 27, 118-123, 2008b. (In Chinese with English abstract)

Wan, R., Zhao, B., and Wu, G.: New evidences on the climatic causes of the formation of the spring persistent rains over southeastern China, Advances in Atmospheric Sciences, 26, 1081-1087, 2009.

Wang, B. and Lin, H.: Rainy season of the Asian–Pacific summer monsoon, Journal of Climate, 15, 386-398, 2002.

Wang, B., Wu, R., and Fu, X.: Pacific–East Asian teleconnection: how does ENSO affect East Asian climate?, Journal of Climate, 13, 1517-1536, 2000.

Wang, Y. Q.: MeteoInfo: GIS software for meteorological data visualization and analysis, Meteorological Applications, 21, 360-368, 2014.

© Author(s) 2018. CC BY 4.0 License.

Wang, Y., Cheng, H., Edwards, R., An, Z., Wu, J., Shen, C., and Dorale, J.: A high-resolution absolute-dated late Pleistocene monsoon record from Hulu Cave, China, Science, 294, 2345, 2001.

Wang, Y., Cheng, H., Edwards, R., Kong, X., Shao, X., Chen, S., Wu, J., Jiang, X., Wang, X., and An, Z.: Millennial-and orbital-scale changes in the East Asian monsoon over the past 224,000 years, Nature, 451, 1090-1093, 2008.

Wang, Y., Zhang, X., and Draxler, R. R.: TrajStat: GIS-based software that uses various trajectory statistical analysis methods to identify potential sources from long-term air pollution measurement data, Environmental Modelling and Software, 24, 938-939, 2009.

Wolter, K., and Timlin, M. S.: El Niño/Southern Oscillation behaviour since 1871 as diagnosed in an extended multivariate ENSO index (MEI. ext), International Journal of Climatology, 31, 1074-1087, 2011.

Wu, H., Zhang, X., Xiaoyan, L., Li, G., and Huang, Y.: Seasonal variations of deuterium and oxygen - 18 isotopes and their response to moisture source for precipitation events in the subtropical monsoon region, Hydrological Processes, 29, 90-102, 2015.

Wu, R. and Kirtman, B. P.: Observed relationship of spring and summer East Asian rainfall with winter and spring Eurasian snow, Journal of Climate, 20, 1285-1304, 2007.

Wu, X. and Mao, J.: Interdecadal modulation of ENSO-related spring rainfall over South China by the Pacific Decadal Oscillation, Climate dynamics, 47, 3203-3220, 2016.

Xu, C., Ge, J., Nakatsuka, T., Yi, L., Zheng, H., and Sano, M.: Potential utility of tree ring $\delta^{18}O$ series for reconstructing precipitation records from the lower reaches of the Yangtze River, southeast China, Journal of Geophysical Research: Atmospheres, 121, 3954-3968, 2016a.

Xu, C., Zheng, H., Nakatsuka, T., and Sano, M.: Oxygen isotope signatures preserved in tree ring cellulose as a proxy for April–September precipitation in Fujian, the subtropical region of southeast China, Journal of Geophysical Research: Atmospheres, 118, 12,805-812,815, 2013.

Xu, C., Zheng, H., Nakatsuka, T., Sano, M., Li, Z., and Ge, J.: Inter-and intra-annual tree-ring cellulose oxygen isotope variability in response to precipitation in Southeast China, Trees, 30, 785-794, 2016b.

Xue, F. and Liu, C.: The influence of moderate ENSO on summer rainfall in eastern China and its comparison with strong ENSO, Chinese Science Bulletin, 53, 791-800, 2008.

Yang, H., Johnson, K., Griffiths, M., and Yoshimura, K.: Interannual controls on oxygen isotope variability in Asian monsoon precipitation and implications for paleoclimate reconstructions, Journal of Geophysical Research: Atmospheres, 121, 8410-8428, 2016.

Yatagai, A., Arakawa, O., Kamiguchi, K., Kawamoto, H., Nodzu, M. I., and Hamada, A.: A 44-year daily gridded precipitation dataset for Asia based on a dense network of rain gauges, Sola, 5, 137-140, 2009.

Yoshimura, K., Kanamitsu, M., Noone, D., and Oki, T.: Historical isotope simulation using reanalysis atmospheric data, Journal of Geophysical Research: Atmospheres, 113, 2008.

© Author(s) 2018. CC BY 4.0 License.

Yuan, D., Cheng, H., Edwards, R., Dykoski, C., Kelly, M., Zhang, M., Qing, J., Lin, Y., Wang, Y., and Wu, J.: Timing, duration, and transitions of the last interglacial Asian monsoon, Science, 304, 575-577, 2004.

Zhang, H., Cheng, H., Spötl, C., Cai, Y., Sinha, A., Tan, L., Yi, L., Yan, H., Kathayat, G., Ning, Y., Li, X., Zhang, F., Zhao, J., and Edwards, R. L.: A 200-year annually laminated stalagmite record of precipitation seasonality in southeastern China and its linkages to ENSO and PDO, Scientific reports, 8, 12344, 2018.

Zhang, H.: The different precipitation patterns in East Asian monsoon region during Holocene, PhD thesis, The University of Chinese Academy of Sciences, 2014. (In Chinese with English abstract)

Zhang, P., Cheng, H., Edwards, R., Chen, F., Wang, Y., Yang, X., Liu, J., Tan, M., and Wang, X.: A test of climate, sun, and culture relationships from an 1810-year Chinese cave record, Science, 322, 940-942, 2008.

Zhang, R., Sumi, A., and Kimoto, M.: A diagnostic study of the impact of El Nino on the precipitation in China, Advances in Atmospheric Sciences, 16, 229-241, 1999.

Zhang, X. P., Guan, H. D., Zhang, X. Z., Wu, H. W., Li, G., and Huang, Y. M.: Simulation of stable water isotopic composition in the atmosphere using an isotopic Atmospheric Water Balance Model, International Journal of Climatology, 35, 846-859, 2015.

Zhou, L. T.: Impact of East Asian winter monsoon on rainfall over southeastern China and its dynamical process, International Journal of Climatology, 31, 677-686, 2011.

Zhou, L.-T. and Wu, R.: Respective impacts of the East Asian winter monsoon and ENSO on winter rainfall in China, Journal of Geophysical Research: Atmospheres, 115, D02107, 2010.

Zhou, W. and Chan, J. C.: ENSO and the South China Sea summer monsoon onset, International Journal of Climatology, 27, 157-167, 2007.